How to cite: *Angew. Chem. Int. Ed.* **2023,** *62,* e202217806
International Edition: doi.org/10.1002/anie.202217806
German Edition: doi.org/10.1002/ange.202217806

Mesoporous Materials

Laser Writing of Block-Copolymer Images into Mesopores Using SBDC-Initiated Visible-Light-Induced Polymerization

*Claire Förster, Robert Lehn, Enis Musa Saritas, and Annette Andrieu-Brunsen**

Abstract: For miniaturization, as well as for improving artificial nanopore performance, precise local polymer functionalization and the combination of different functionalities are required. Imagining data driven nanopore design automated nanopore functionalization would be beneficial. Using direct laser writing as one option of automated nanopore polymer functionalization visible light induced polymerizations are beneficial. Here, we demonstrate the functionalization of mesoporous silicafilms with two different polymers using automated laser writing. For this we developed a visible light (400–700 nm and 405 nm) *N*,*N*-(diethylamino)dithiocarbamoylbenzyl(trimethoxy)silane (SBDC) inifierter initiated polymerization. While transferring this visible light induced polymerization using SBDC to a commercially available microscope, direct, automated laser writing, as well as polymer re-initiation was demonstrated. Thereby, polymer spots of 37 and 40 µm in diameter were achieved using 1–5 seconds for each irradiated spot.

Introduction

Micro- and nanostructures have become increasingly important in many applications in recent years. One commonly used way to manipulate the attributes of micro- and nanostructures is their surface functionalization using polymers. Light-induced polymerizations allow for spatial and temporal control over chemical reactions and especially control over polymer chain growth. In many applications, such as cell cultures,[1] artificial tissue engineering[2] or biomedical implants[3] the use of visible light instead of UV light is advantageous.[4] Visible light is also considered to promote wound healing,[5] which is particularly advantageous for the mentioned examples.[6] Furthermore, visible light is considered to be one part of greener chemistry as it can be provided by nature directly.[7] These advantages of visible light motivate the investigation of visible light-based chemical reactions and functionalization, especially in the field of polymerization and polymer functionalization of interfaces. Most light-induced processes are using mask-based lithography, which makes them time effecient.[8] Nevertheless, the non-flexible nature of mask-based photolithography processes makes them less desirable in case rapid prototyping is required. Alternative techniques for polymer structuring, based e.g. on electron beam,[9] scanning probe[10] or two-photon processes[11] were developed. Furthermore, direct laser writing (DLW), which is often based on two-photon processes, opens flexibility for local polymer functionalization. Especially with respect to functionalization in three dimensions DLW techniques are promising and frequently used.[6,12] In general, for laser induced polymer writing, simple reaction conditions and short irradiation times are preferred. One frequently occurring difficulty in the context of polymer functionalization is the intolerance towards oxygen. The deoxygenation, for example by freeze-pump-thaw cycles or the use of a glovebox can be time and cost intensive and incompatible with DLW. In 1998 Matyjaszewski et al. reported one of the first oxygen tolerant controlled radical polymerizations (CRPs).[13] Since then different approaches were developed to achieve oxygen tolerant CRPs. Examples are the use of glucose oxidase (GOx) which consumes the oxygen before the polymerization,[14] the use of reducing agents[15] as well as inducing the conversion from molecular to singulett oxygen and subsequent trapping of the reactive oxygen species.[16] A full overview on oxygen tolerance in CRPs has been given by Boyer.[17] In addition to simple experimental conditions, such as oxygen tolerance, the fabrication of more complex surfaces is one aspect of current research[18] which is of interest for the functionalization of nanopores. Especially, local functionalization and precise placement of different functional polymers or bock copolymer formation is a promising approach to the design of nanopore performance with respect to nanopore transport. For example, theoretical studies from Szleifer and colleagues[19,20] demonstrate the importance of precise nanopore functionalization, as well as polymer sequence control for directed and selective ion transport. In an experimental study Azzaroni and colleagues achieved a thermosensitive cation-selective mesochannel using local polymer functionalization only on the outer surface of the mesoporous silicafilm. The precise functionalization was achieved using an iniferter, which was surface-anchored by its Z-group.[21] Our research group demon-

[*] C. Förster, Dr. R. Lehn, E. M. Saritas, Prof. Dr. A. Andrieu-Brunsen
Ernst-Berl Institut für Technische und Makromolekulare Chemie
Technische Universität Darmstadt
Alarich-Weiss-Strasse 8, 64287 Darmstadt (Germany)
E-mail: annette.andrieu-brunsen@tu-darmstadt.de

strated for example layer selective polymer functionalization in multilayer mesoporous films.[22] Until now the experimental functionalizations of nanoscale pores are mostly limited to homopolymers. Re-initiation using CRPs in nanoscale pores was only achieved recently using the photoiniferter *N*,*N*(diethylamino)dithiocarbamoylbenzyl(trimethoxy)silane (SBDC)[23,24] as well as photo electron/energy transfer (PET)—Reversible Addition Fragmentation chain Transfer RAFT polymerization.[25] Using SBDC as iniferter on planar surfaces, Rahane et al.[26] analyzed the kinetics of methylmethacrylates under 365 nm light irradiation. Also using 365 nm light, de Boer et al.[27] functionalized surfaces with styrol and methylmethacrylate. Under UV irradiation, the initiation of the polymerization is based on the hetrerolytic dissociation of SBDC.[28] This heterolytic dissociation of the basic structure of SBDC, benzyl diethyldithiocarbamate (BDC), under the influence of light was first described by Okawara et al. in 1964.[29] To our knowledge SBDC has not been investigated under visible light irradiation, which would be beneficial to be applied to direct laser writing. Iniferters have been used as chain transfer agents in a visible light induced PET-RAFT polymerization. For example the UV-Iniferter DDMAT (2-(Dodecylthiocarbonothioylthio)-2-methylpropanoic acid)[30] can be used for a visible light induced PET-RAFT[31] through the addition of a photo catalyst. In recent years, the reduction or even avoidance of metal catalysts becomes more and more requested which drives research towards metal-free visible light induced polymerization.

In this study we demonstrate the first example of polymer functionalization of mesoporous silica films ($\approx$13 nm pore diameter) using the iniferter SBDC under visible light irradiation in the absence of any metal-containing photo-catalyst and in the presence of oxygen including polymerization re-initiation and block-copolymer formation and its use in automated polymer writing. ATR-IR and ellipsometry data confirm the successful polymer functionalization under visible light irradiation with and even without additional photo catalyst and thus under metal-free visible light polymerization. Transport behavior of positively and negatively charged probe molecules in these block-copolymer functionalized mesoporous silica films using cyclic voltammetry show the pore accessibility at pH 10 even after functionalization with positively charged polymer. This polymerization was transferred to laser-induced block-copolymer writing of microscale structures using visible light (405 nm) SBDC-initiated polymerization in mesoporous films on a commercially available microscope (Nikon Ti2-E with N-Storm unit) resulting in direct laser writing of a 103×30 pixel sized image. Each pixel represented a polymer spot containing either poly-2-dimethylamino)ethyl methacrylate (PDMAEMA), poly-[2-(methacryloyloxy)ethyl] trimethylammonium chloride (PMETAC) or the PDMAEMA-co-PMETAC block-copolymer.

Results and Discussion

Mesoporous silica films, which were obtained via sol-gel chemistry and evaporation-induced self-assembly (EISA[32]), were functionalized using an easy, oxygen tolerant, and visible light induced SBDC-initiated polymerization. To demonstrate the visible light induced mesopore functionalization with PDMAEMA the polymerization was performed under visible light irradiation (400–700 nm) using SBDC with and without the additional photo catalyst 5,10,15,20-Tetraphenyl-21*H*,23*H*-porphine zinc (ZnTPP, Figure 1). To investigate the potential of visible light induced SBDC-initiated polymerization in context of polymer writing, the polymer amount in dependence of different reaction conditions, such as irradiation time and intensity, as well as irradiation wavelengths, presence, and absence of the photo catalyst ZnTPP, and the influence of the outer surface was investigated. All polymerization experiments were performed in the presence of oxygen. The oxygen tolerance in presence of ZnTPP is explained by the conversion of triplet oxygen to singlet oxygen, which is irreversibly trapped by the DMSO solvent.[17] Without ZnTPP the polymerization may perform a "polymerizing through oxygen", where oxygen reacts with excess radicals in the system.[17,33]

Influence of different light intensities and wavelengths on the polymer amount

The PDMAEMA amount was monitored using ATR-IR spectroscopy upon variation of irradiation time and intensity, as well as presence of the photo catalyst ZnTPP, and functionalization of the outer film surface. PDMAEMA was detected at all applied polymerization conditions, even after 10 min irradiation time (Figure 2a, b, d, e). In the presence of the photo catalyst ZnTPP, the aspects such as a second radical initiating mechanism,[34] confinement effects, and mass transport inside the pores have to be considered. For this reason, in general controlled polymerization with ideally only one initiator and without additional catalysts would be preferred inside nanopores. Analyzing the effect of the presence of ZnTTP on the generated polymer amount for an irradiation intensity of 2.5 mW cm^{-2} and for relatively short irradiation times up to 60 minutes (Figure 2b) interestingly revealed that slightly less polymer was formed in the presence of the photo catalyst.For all other applied conditions no significant effect on the polymer amount was observed within the accuracy of the experiment (Figure 2a, d, e, g, h). Furthermore, increasing the irradiation intensity from 2.5 mW cm^{-2} to 38 mW cm^{-2}, does not result in a significantly different increase of the carbonyl vibrational band at 1720–1730 cm^{-1} (Figure 2a, b, d, e) for polymerization times up to 300 minutes. Estimating the pore filling degrees from the refractive index increase as detected by ellipsometry according to Brüggemann effective medium approximation[41,42] pore filling degrees of up to 90 vol % were obtained. In accordance with ATR-IR data the pore filling degrees increase similarly with irradiation time independently of using 2.5 mW cm^{-2} or 38 mW cm^{-2} (Fig-

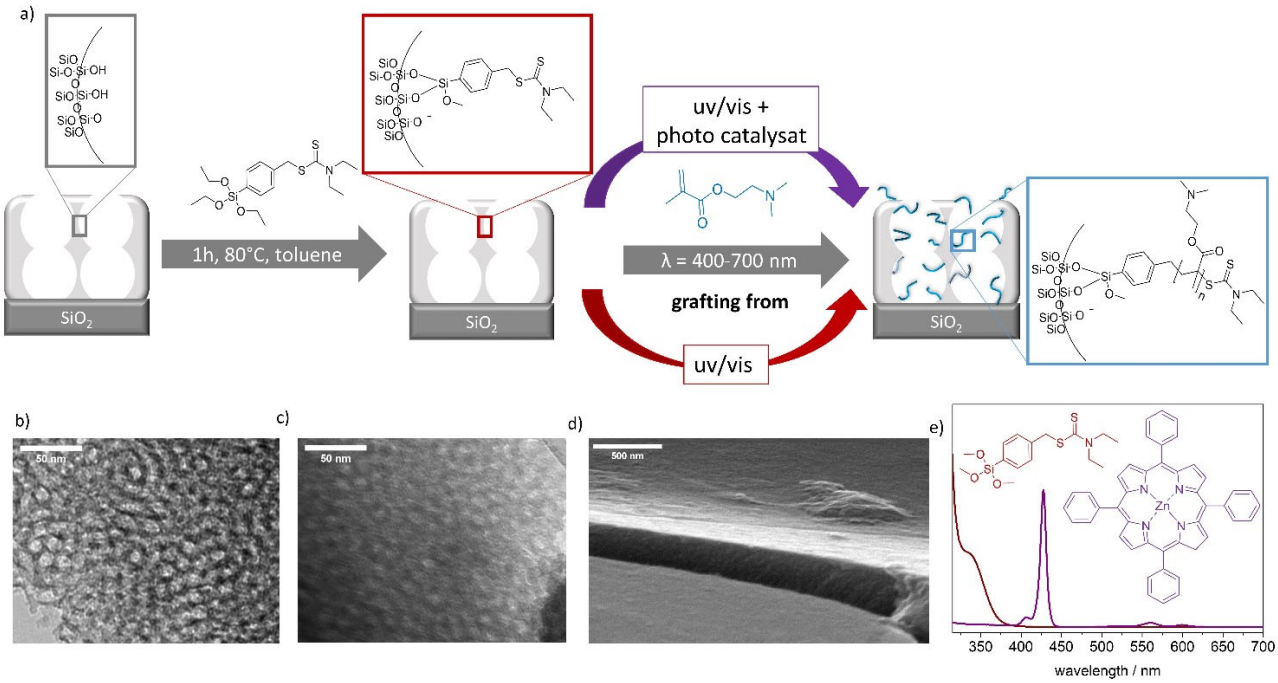

Figure 1. a) Visible light induced polymerization using SBDC to functionalize mesoporous silica thin films (≈500–600 nm) with PDMAEMA. b) TEM image of a mesoporous silica film with pore sizes of ≈13 nm. c) + d) TEM and SEM images of PDMAEMA functionalized mesoporous silica film (3 h polymerization time, using photo catalyst ZnTPP, shows that the film survives the reaction conditions well and has no defects). The SEM image (d) shows a cross-section of the PDMAEMA functionalized mesoporous silica film. e) uv/vis spectra (baseline corrected) of the iniferter SBDC (red) and the photo catalyst ZnTPP (purple) in DMSO.

ure 2f, Table S2–Table S11). This observation indicates that visible light induced polymerization and polymer writing with SBDC as initiator is possible even without photocatalyst.

Furthermore, CO_2-plasma[35,36] treated mesoporous films, which do not allow polymer growth on the outer mesoporous film surface due to the destruction of the initiator, show similar time and irradiation energy, as well as wavelength (365 nm and 400–700 nm, Figure 2a, d, g) dependent polymer amount as mesoporous films without CO_2-plasma treatment. Additionally, a similar maximum polymer amount, with approximately 0.15 a.u. carbonyl vibrational band intensity, was observed for all investigated polymerization conditions (Figure 2a, b, d, e, g, h). The intensity of the carbonyl vibrational band at approximately 1720–1730 cm^{-1} in normalized ATR-IR spectra of approx. 0.15 a.u. correlates to pore filling degrees of approximately 80 vol % according to ellipsometry data (Figure 2f). This indicates that the polymerization predominantly seems to take place inside of the mesopores, independently from the CO_2-plasma treatment. This observation of polymerization mainly occurring inside the mesoporous film but not on the outer planar surface together with TEM and EDX mapping of a previous study of our group[37] indicates that diffusion of the cleaved SBDC initiator from the outer surface into the surrounding solution interrupts the polymerization at the outer mesoporous film surface, whereas the diffusion of cleaved SBDC out of the mesopores seems to be less favored resulting in progression of the polymerization reaction. This is an interesting observation as this allows polymerization inside the mesopores without any further processing step.

Re-initiation with METAC and ionic pore accessibility

After a first metal free visible light and SBDC-initiated polymerization in mesoporous silica films re-initiation was achieved and block-copolymers of PDMAEMA-*b*-PMETAC were synthesized (Figure 3a, c). PMETAC is a positively charged, strong polyelectrolyte. As PDMAEMA can also carry a positive charge with a pK_a value in solution of around pH 7.5[39] the re-initiation was carried out at two different pH values of pH 6 and pH 9. We observed a 1.7 times higher polymer amount at pH 9 at which PDMAEMA is expected to be neutrally charged as compared to pH 6 using 10 minutes polymerization time at 38 mW cm^{-2} irradiation intensity (Figure S4). For the PDMAEMA-*b*-PMETAC block-copolymer functionalization the mesoporous silica films were functionalized with PDMAEMA using visible light irradiation for 10 min at 38 mW cm^{-2} without additional photo catalyst. The PDMAEMA functionalization results in an intensity of the carbonyl vibrational band of approximately 0.03 a.u. and pore filling degrees of 24–49 % (Figure 3b, Table S11–Table S13). Subsequent re-initiation using METAC was performed in the presence of the photo catalyst ZnTPP under visible light irradiation. The monomer METAC was used without previous destabilization. Upon re-initiation using METAC and ZnTPP for

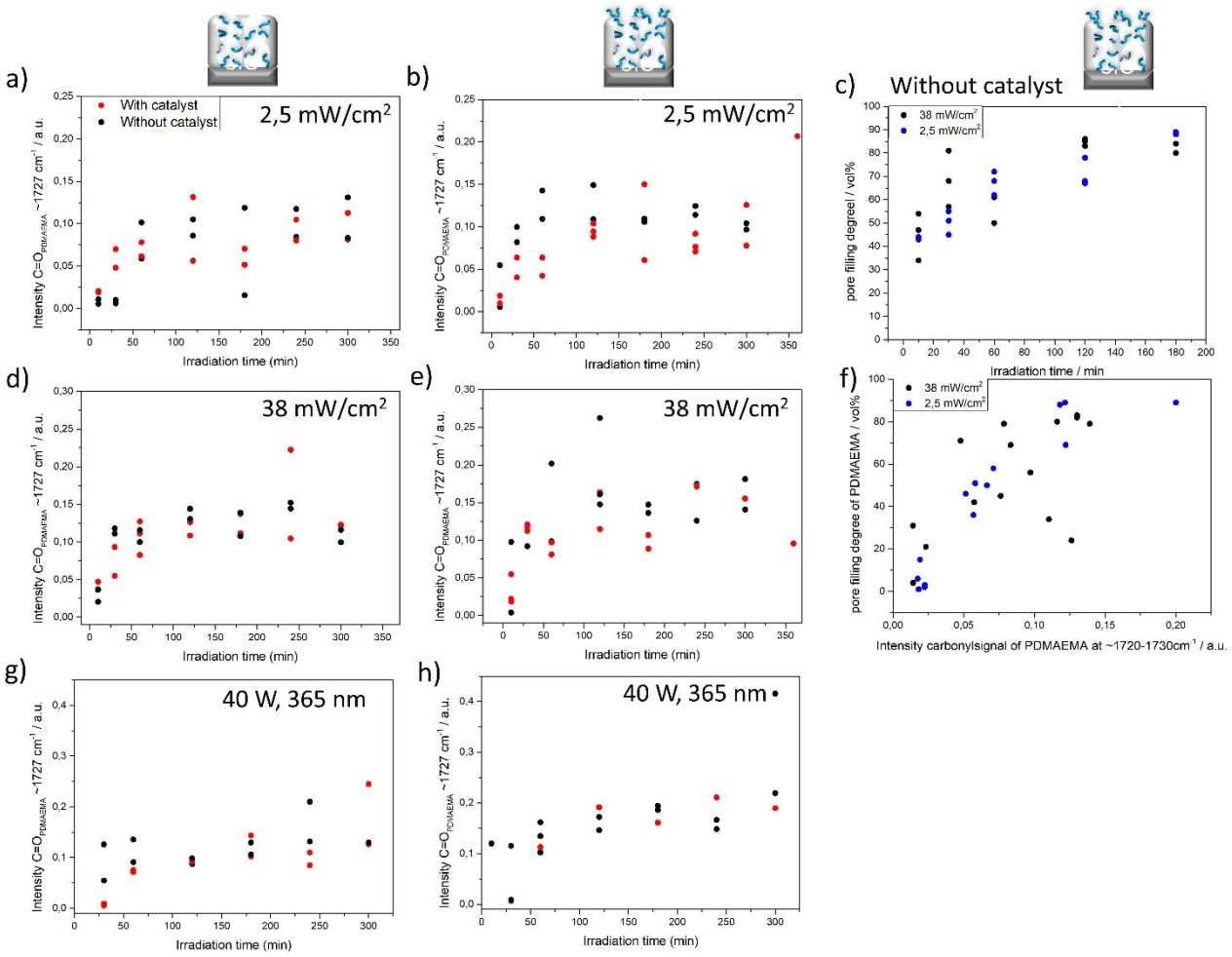

Figure 2. Influence of varying irradiation intensities and irradiation wavelengths on the polymer amount in mesoporous silica films. a), b), d), e), g), h) Normalized intensities of the carbonyl vibrational band of PDMAEMA at 1720 cm^{-1} in dependence of the irradiation time, analyzed in Si–O–Si–VS (approximately 1060 cm^{-1}) normalized ATR-IR spectra using mesoporous films after being scratched off from the supporting substrate. The different data points in Figure 2 which shows the results of ATR-IR measurements, are based on multiple performance of the polymerization-experiment. a–f) Polymerization using visible light (400–700 nm) under the following specific parameter variations: a) 2.5 mW cm^{-2}, with CO_2 plasma treatment, b) 2.5 mW cm^{-2}, without CO_2 plasma treatment, d) 38 mW cm^{-2}, with CO_2 plasma treatment, e) 38 mW cm^{-2}, without CO_2 plasma treatment. g + h) Polymerization using UV-light (365 nm) for g) mesoporous films treated with CO_2 plasma before polymerization and h) mesoporous films without CO_2 plasma treatment. c), f) Results of ellipsometry measurements from Iniferter initiated polymerization using SBDC without catalyst, at 38 (black) and 2.5 (blue) mW cm^{-2} without CO_2 plasma treatment. Pore filling degrees in dependence of irradiation time. f) Correlation between pore filling degree of PDMAEMA and the intensity of the carbonylsignal from ATR-IR measurements.

10 min at 38 mW cm^{-2} the intensity of the carbonyl vibrational band increased to approximately 0.07 a.u. and high pore filling degrees up to 100 vol % were obtained (Figure 3b, Table S11–Table S13) as deduced from ellipsometry and refractive index increase. An irradiation time longer than 10 minutes during re-initiation with METAC results only in a small further increase of the carbonyl vibrational band up to 0.10 a.u. (Figure 3c).

Block-copolymer chain architectures in mesopores have been predicted to show interesting transport properties.[19] A first comparison of our research group between zwitterionic and counter charged block-oligomer functionalization of nanopores reveals an influence of the chain architecture on the observed ionic pore accessibility.[24,40] The ionic pore accessibility was analyzed using cyclic voltammetry (CV, Figure 4). The unmodified mesoporous silica film shows, as expected, a good accessibility for the positively charged $[Ru(NH_3)_6]^{2+/3}$ at pH 10 (Figure 4a, red). The negatively charged $[Fe(CN)_6]^{3-/4-}$ shows exclusion at basic pH due to the negatively charged silanol groups (Figure 4a, purple). In contrast, the PDMAEMA-*b*-PMETAC functionalized silica film shows pore accessibility of the negatively charged $[Fe(CN)_6]^{3-/4-}$ even at basic conditions, at which the remaining silanol groups of the mesoporous silica film is expected to be negatively charged. This indicates the presence of positive charges from the polymer chains grafted from the mesopore wall. The pore accessibility of the positively charged $[Ru(NH_3)_6]^{2+/3}$ is significantly reduced and these ions are almost excluded from the PDMAEMA-*b*-PMETAC functionalized mesopores even at basic pH at

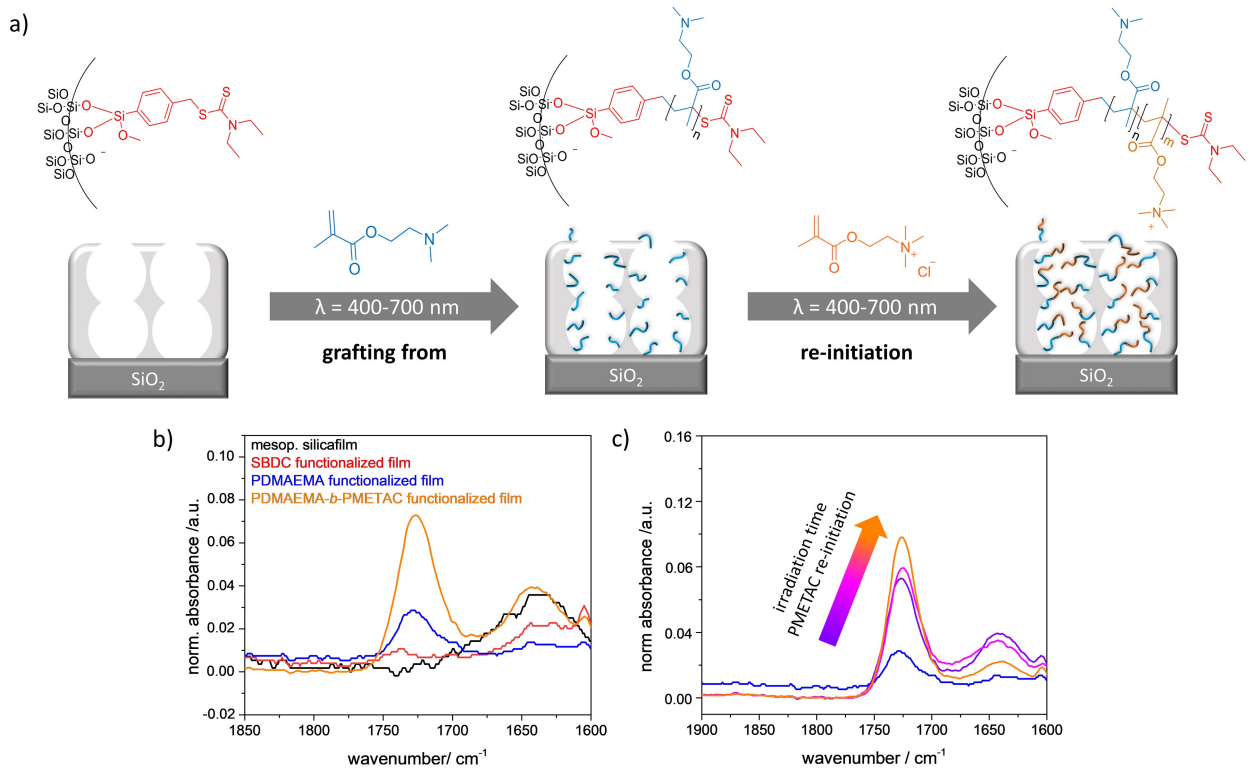

Figure 3. a) Schematic illustration of PDMAEMA-*b*-PMETAC functionalization of mesoporous silica films upon re-initiation. b) Zoom of the C=O– vibrational band of the ATR-IR spectra of PDMAEMA-*b*-PMETAC functionalized films after each functionalization step. c) The C=O vibrational band after different irradiation times for the re-initiation with METAC after PDMAEMA functionalization for 10 min (blue); (purple) 10 min; (magenta) 30 min; (orange) 60 min irradiation for PMETAC re-initiation. The zoom (b + c) also shows the valence vibrations of H_2O at approximately 1640 cm^{-1} originating from absorbed water molecules to the silica film.[38]

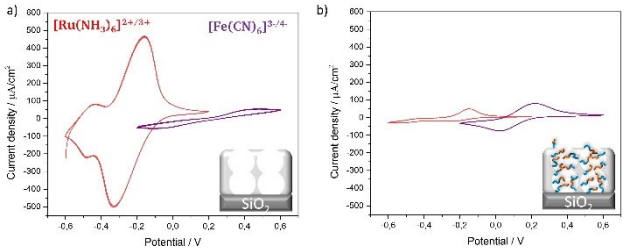

Figure 4. CV measurements of a) unmodified mesoporous silica film and b) PDMAEMA-*b*-PMETAC functionalized mesopores silica films. Red) positively charged probe molecule $[Ru(NH_3)_6]^{2+/3+}$ at pH 10, purple) negatively charged probe molecule $[Fe(CN)_6]^{3-/4-}$ at pH 10. Concentration of probe molecules: 1 mM in 100 mM KCl electrolyte solution.

which pre-concentration is observed without polymer functionalization (Figure 4b). The PDMAEMA block is expected to be neutrally charged at pH 10 (pK_a value of PDMAEMA in solution around pH 7.5),[39] why the exclusion of cations is ascribed to the positively charged PMETAC supporting the presence of both blocks after polymerization re-initiation.

Direct laser writing for local polymer functionalization in mesopores

The oxygen tolerant nature of PET-RAFT with SBDC and especially the observation of visible light induced polymerization even without photocatalyst as well as the use of visible light for initiation due to the presence of ZnTPP even for stabilized METAC, favors a transfer of this reaction to automated polymer writing in mesoporous films or coatings using a commercially available microscope for local laser illumination. This would enable local direct laser writing in mesoporous silica films. As a proof-of-concept study, a 103 × 30 pixel sized image was written into a mesoporous silica film using SBDC-initiated PET-RAFT of DMAEMA and METAC. The size of the achieved polymer spots was 37 µm in diameter for PDMAEMA and 41 µm for PMETAC while using an irradiation laser beam with a size of 41 µm in diameter ($1/e^2$). Following the achieved spot size, the distance between spots was set to 40 µm. For PDMAEMA, the laser power was set to 50 mW (approximately 416 $W\,cm^{-2}$) and an irradiation time of 5 seconds per spot was chosen. PMETAC was polymerized with a laser power of 20 mW (approximately 190 $W\,cm^{-2}$) and 1 second of irradiation. The values for power and time were chosen to create polymer spots with roughly the same size for both polymers, while also being the same size as the illumination beam. As observed for a different polymerization

mechanism,[43] the size of the written polymer spot can be tuned down with modulation of irradiation time and power to a much lower size compared to the used irradiation laser beam which was not optimized in this study, yet. After polymerization, the sample was stained, first, with Alexa Fluor 488 (1 mg L^{-1}) and then ATTO647N (1 mg L^{-1}), both at neutral pH. The negatively charged Alexa Fluor 488 adsorbs to the positively charged PMETAC, while the positively charged ATTO647N adsorbs to the non-functionalized silicafilm. A final washing step with water at pH 4 proved to be very beneficial for image clarity. The stained sample was then imaged with a confocal laser scanning microscope (Leica SP8). Figure 5 shows the possibility to use multiple monomers in the same sample and the ability to re-initiate polymerization at previously functionalized areas.

Overall, the sample shown in Figure 5 consists of 1494 PDMAEMA (black) and 437 PMETAC (green) spots. The combined illumination time was 2.2 hours. The zoom clearly shows re-initiation of polymerization in areas where the black and the green spots overlap. The grid of the illumination pattern was slightly moved between polymerization of PDMAEMA and PMETAC to better show only partly overlapping polymer spots.

Together, this shows that SBDC is a capable iniferter for oxygen tolerant, visible light-induced PET-RAFT with and without photocatalyst ZnTPP. It can be used for polymerization re-initiation and the creation of block-copolymers in a micro-local fashion in mesoporous silica film.

Conclusion

We demonstrated the first example of mesopore functionalization using the iniferter SBDC under visible light irradiation at 405 nm even without additional photocatalyst. Furthermore, we demonstrate the use of this visible light induced SBDC-initiated polymerization for automated micrometer scale polymer and block copolymer writing into mesoporous silica layers. The amount of PDMAEMA functionalization in mesopores was investigated and optimized towards microscope-based automated polymer and block-copolymer writing under varying polymerization conditions, such as the presence and absence of the photo catalyst ZnTPP, CO_2-plasma[35,36] treatment, and different polymerization irradiation intensities. In this context we found that polymer amount can be varied even for short irradiation times and that under all investigated conditions, the maximum amount of polymer detectable in the ATR-IR corresponds to a pore filling degree of approximately 90 vol %. In accordance with a previous study,[37] these results indicate a diffusion of the cleaved SBDC initiator from the outer surface into the surrounding solution terminating the polymerization at the outer surface. Through such a polymerization-disrupting diffusion on the outer surface, functionalities can be easily achieved only within the mesopores without additional steps, such as CO_2-plasma[35,36] treatment. Importantly, polymerization re-initiation using this visible light SBDC-initiated polymerization was demonstrated, and resulting ionic pore accessibility at basic pH even after functionalization with positively charged polymers was observed. This polymerization development finally enabled the combination of this visible light SBDC-initiated polymerization with a commercially available microscope (Nikon Ti2-E with N-Storm unit) to write multifunctional micrometer scale polymer and block-copolymer images into mesopores demonstrating automated, multifunctional local and well-resolved laser writing in ≈13 nm pores. This opens a door towards high throughput and automated polymer-mesoporous ceramic hybrid material fabrication with high local resolution and multifunctionality.

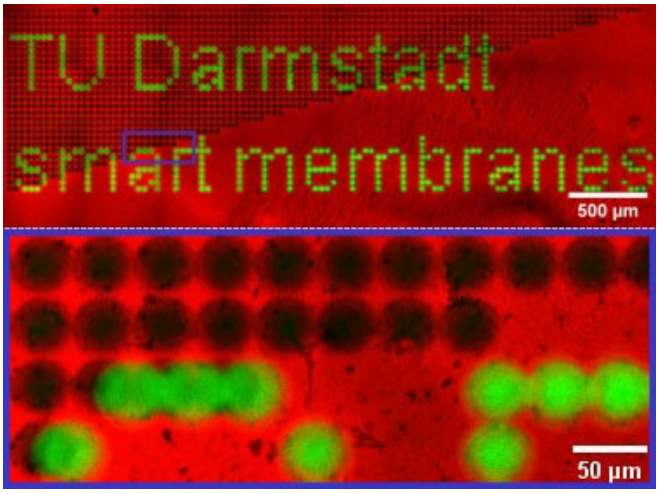

Figure 5. Confocal laser scanning image of PDMAEMA and PMETAC multi-functionalized mesoporous silica film. PMETAC is visualized by staining with Alexa Fluor 488 due to opposite charge (green). Non-functionalized mesoporous silica film is shown by staining with ATTO647N (red). DMAEMA is indirectly shown by exclusion of ATTO647N in functionalized areas (black).

Acknowledgements

The authors acknowledge funding from the European Research Council (ERC) under the European Union's Horizon 2020 research and innovation program (grant agreement No 803758). The authors further thank Ulrike Kunz and Prof. Kleebe (TU-Darmstadt) for TEM measurements and the research group of Biesalski (TU-Darmstadt) for access to the TGA. Sandra Pietrasch is acknowledged for support in performing cyclic voltammetry measurements. Open Access funding enabled and organized by Projekt DEAL.

Conflict of Interest

The authors declare no conflict of interest.

Data Availability Statement

The data that support the findings of this study are available from the corresponding author upon reasonable request.

Keywords: Automated Polymer Writing · Iniferter Initiated Polymerization · Laser Induced Polymerization · Mesoporous Silica · Visible Light-Induced Polymerization

[1] a) V. Melissinaki, A. A. Gill, I. Ortega, M. Vamvakaki, A. Ranella, J. W. Haycock, C. Fotakis, M. Farsari, F. Claeyssens, *Biofabrication* **2011**, *3*, 045005; b) S. Selimović, F. Piraino, H. Bae, M. Rasponi, A. Redaelli, A. Khademhosseini, *Lab Chip* **2011**, *11*, 2325.
[2] a) M. Malinauskas, D. Baltriukiene, A. Kraniauskas, P. Danilevicius, R. Jarasiene, R. Sirmenis, A. Zukauskas, E. Balciunas, V. Purlys, R. Gadonas, et al., *Appl. Phys. A* **2012**, *108*, 751; b) P. Danilevicius, S. Rekstyte, E. Balciunas, A. Kraniauskas, R. Jarasiene, R. Sirmenis, D. Baltriukiene, V. Bukelskiene, R. Gadonas, M. Malinauskas, *J. Biomed. Opt.* **2012**, *17*, 081405.
[3] S. Galanopoulos, N. Chatzidai, V. Melissinaki, A. Selimis, C. Schizas, M. Farsari, D. Karalekas, *Micromachines* **2014**, *5*, 505.
[4] J. Wei, R. Wang, *J. Appl. Phys.* **2014**, *115*, 123102.
[5] S.-J. Yoon, H. Hyun, D.-W. Lee, D. H. Yang, *Molecules* **2017**, *22*, 1513.
[6] H. Yu, H. Ding, Q. Zhang, Z. Gu, M. Gu, *gxjzz* **2021**, *2*, 31.
[7] a) G. E. M. Crisenza, P. Melchiorre, *Nat. Commun.* **2020**, *11*, 803; b) T. P. Yoon, M. A. Ischay, J. Du, *Nat. Chem.* **2010**, *2*, 527; c) C. A. Boyer, G. M. Miyake, *Macromol. Rapid Commun.* **2017**, *38*, 1700327.
[8] J. Rühe, *ACS Nano* **2017**, *11*, 8537.
[9] a) P. Ruchhoeft, J. C. Wolfe, R. Bass, *J. Vac. Sci. Technol. B* **2001**, *19*, 2529; b) C. Vieu, F. Carcenac, A. Pépin, Y. Chen, M. Mejias, A. Lebib, L. Manin-Ferlazzo, L. Couraud, H. Launois, *Appl. Surf. Sci.* **2000**, *164*, 111.
[10] A. A. Tseng, A. Notargiacomo, T. P. Chen, *J. Vac. Sci. Technol. B* **2005**, *23*, 877.
[11] K.-S. Lee, R. H. Kim, D.-Y. Yang, S. H. Park, *Prog. Polym. Sci.* **2008**, *33*, 631.
[12] a) H.-B. Sun, S. Matsuo, H. Misawa, *Appl. Phys. Lett.* **1999**, *74*, 786; b) A. Selimis, V. Mironov, M. Farsari, *Microelectron. Eng.* **2015**, *132*, 83; c) M. Malinauskas, M. Farsari, A. Piskarskas, S. Juodkazis, *Phys. Rep.* **2013**, *533*, 1.
[13] K. Matyjaszewski, S. Coca, S. G. Gaynor, M. Wei, B. E. Woodworth, *Macromolecules* **1998**, *31*, 5967.
[14] a) R. Chapman, A. J. Gormley, K.-L. Herpoldt, M. M. Stevens, *Macromolecules* **2014**, *47*, 8541; b) A. E. Enciso, L. Fu, A. J. Russell, K. Matyjaszewski, *Angew. Chem. Int. Ed.* **2018**, *57*, 933; *Angew. Chem.* **2018**, *130*, 945.
[15] a) W. Jakubowski, K. Min, K. Matyjaszewski, *Macromolecules* **2006**, *39*, 39; b) S. Fleischmann, V. Percec, *J. Polym. Sci. Part A* **2010**, *48*, 2243.
[16] a) S. Shanmugam, J. Xu, C. Boyer, *J. Am. Chem. Soc.* **2015**, *137*, 9174; b) N. Corrigan, D. Rosli, J. W. J. Jones, J. Xu, C. Boyer, *Macromolecules* **2016**, *49*, 6779.
[17] J. Yeow, R. Chapman, A. J. Gormley, C. Boyer, *Chem. Soc. Rev.* **2018**, *47*, 4357.
[18] R. Brilmayer, C. Förster, L. Zhao, A. Andrieu-Brunsen, *Curr. Opin. Biotechnol.* **2020**, *63*, 200.
[19] K. Huang, I. Szleifer, *J. Am. Chem. Soc.* **2017**, *139*, 6422.
[20] S. Qin, K. Huang, I. Szleifer, *ACS Nano* **2021**, *15, 11, 17678–17688*. DOI: 10.1021/acsnano.1c05543
[21] S. Schmidt, S. Alberti, P. Vana, G. J. A. A. Soler-Illia, O. Azzaroni, *Chem. Eur. J.* **2017**, *23*, 14500.
[22] J. C. Tom, C. Appel, A. Andrieu-Brunsen, *Soft Matter* **2019**, *15*, 8077.
[23] J. C. Tom, R. Brilmayer, J. Schmidt, A. Andrieu-Brunsen, *Polymer* **2017**, *9*, 539. DOI: 10.3390/polym9100539
[24] R. Brilmayer, C. Hess, A. Andrieu-Brunsen, *Small* **2019**, *15*, 1902710.
[25] C. Förster, L. Veith, A. Andrieu-Brunsen, *RSC Adv.* **2022**, *12*, 27109.
[26] S. B. Rahane, S. M. Kilbey, A. T. Metters, *Macromolecules* **2005**, *38*, 8202.
[27] B. de Boer, H. K. Simon, M. P. L. Werts, E. W. van der Vegte, G. Hadziioannou, *Macromolecules* **2000**, *33*, 349.
[28] T. Otsu, *J. Polym. Sci. Part A* **2000**, *38*, 2121.
[29] M. Okawara, T. Nakai, K. Morishita, E. Imoto, *Zasshi* **1964**, *67*, 2108.
[30] H. Wang, Q. Li, J. Dai, F. Du, H. Zheng, R. Bai, *Macromolecules* **2013**, *46*, 2576.
[31] a) M. Li, M. Fromel, D. Ranaweera, S. Rocha, C. Boyer, C. W. Pester, *ACS Macro Lett.* **2019**, *8*, 374; b) G. Li, W. Feng, N. Corrigan, C. Boyer, X. Wang, J. Xu, *Polym. Chem.* **2018**, *9*, 2733.
[32] C. J. Brinker, Y. Lu, A. Sellinger, H. Fan, *Adv. Mater.* **1999**, *11*, 579.
[33] J. R. Lamb, K. P. Qin, J. A. Johnson, *Polym. Chem.* **2019**, *10*, 1585.
[34] M. L. Allegrezza, D. Konkolewicz, *ACS Macro Lett.* **2021**, *10*, 433.
[35] F. Krohm, J. Kind, R. Savka, M. Alcaraz Janßen, D. Herold, H. Plenio, C. M. Thiele, A. Andrieu-Brunsen, *J. Mater. Chem. C* **2016**, *4*, 4067.
[36] D. J. Babu, S. Yadav, T. Heinlein, G. Cherkashinin, J. J. Schneider, *J. Phys. Chem. C* **2014**, *118*, 12028.
[37] R. Brilmayer, S. Kübelbeck, A. Khalil, M. Brodrecht, U. Kunz, H.-J. Kleebe, G. Buntkowsky, G. Baier, A. Andrieu-Brunsen, *Adv. Mater. Interfaces* **2020**, *7*, 1901914.
[38] a) A. Calvo, P. C. Angelomé, V. M. Sánchez, D. A. Scherlis, F. J. Williams, G. J. A. A. Soler-Illia, *Chem. Mater.* **2008**, *20*, 4661; b) M. Hesse, H. Meier, B. Zeeh, *Spektroskopische Methoden in der organischen Chemie. 102 Tabellen*, Thieme, Stuttgart, **2005**.
[39] P. van de Wetering, N. J. Zuidam, M. J. van Steenbergen, O. A. G. J. van der Houwen, W. J. M. Underberg, W. E. Hennink, *Macromolecules* **1998**, *31*, 8063.
[40] L. Silies, A. Andrieu-Brunsen, *Langmuir* **2018**, *34*, 807.
[41] J. E. Spanier, I. P. Herman, *Physical Review B* **2000**, *61*, 10437.
[42] C. Boissiere, D. Grosso, S. Lepoutre, L. Nicole, A. B. Bruneau, C. Sanchez, *Langmuir* **2005**, *21*, 12362.
[43] C. Förster, R. Lehn, A. Andrieu-Brunsen, *Small* **2023**, *19*, 2207762.

Manuscript received: December 2, 2022
Accepted manuscript online: March 15, 2023
Version of record online: March 29, 2023